

Ring templated nanochannel architecture of imidazolium phosphonoacetate

Veneta Videnova-Adrabińska

Institute of Inorganic Chemistry and Metallurgy of Rare Elements, Wrocław University of Technology, 23 Smoluchowskiego St, 50-370 Wrocław, Poland.

E-mail: veneta@ichn.ch.pwr.wroc.pl

Received 27th February 2002, Accepted 19th June 2002

First published as an Advance Article on the web 16th August 2002

The supramolecular architecture of imidazolium phosphonoacetate is shown to consist of anionic monolayers that are parallel stacked in the third direction in order to form channels in which the cations are organized. The two-dimensional hydrogen-bonded network, formed *via* two O–H···O interactions, is characterized by large, nano-size cavities that are surrounded by six phosphonoacetate residues. The imidazolium residues fit in the cavities and connect the monolayers *via* two N–H···O hydrogen bonds. Weak C–H···O interactions additionally stabilize the channel architecture, locking the imidazolium rings. The rings are intercalated in the channels at a unit cell distance and no stacking or other aromatic interactions exist between them.

Introduction

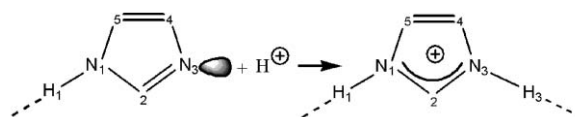
The design and synthesis of specific supramolecular architectures continues to be a theme of current interest in the context of developing materials with particular features and desired optical, electrical or catalytic properties. Considerable progress has been made during the last ten years in controlling the assemblies and the orientation of the individual molecules in them.¹ Hydrogen bonding has been recognized as the most powerful directional force and this aggregates molecules in a quite predictable manner using recurring hydrogen-bonded patterns (synthons).² The use of a variety of structural modules and/or their combinations for the generation of one- and two-dimensional networks has become an important strategy in organic crystal engineering. However the search for elaborate routes giving reliable molecular organization in predictable crystal structures is still elusive and disappointing, mostly due to the numerous weak intermolecular interactions leading to a multiplicity of structural possibilities. The crystal, considered as an ideal ‘*supermolecule*’ dictates a fine balance between attractive forces and stabilization energy and, thus, demands an efficient compromise between molecular arrangements and crystal symmetry constraints. The non-specific, and therefore difficult to control, weak intermolecular interactions are of primary concern owing to their decisive role in the close-packing process.

An attractive way to overcome the dilemma of weak interactions in order to achieve maximum stabilization of the lattice is to use a combination of hydrogen bonding and ionic interactions since the hydrogen bond strength accompanied by an ionic component ranges between 40 and 190 kJ mol⁻¹ compared to 10–65 kJ mol⁻¹ for hydrogen bonds between neutral molecules. Recognizing the potential of this approach, we have embarked on a program aimed at the topological predisposition and the mutual steric and geometric compatibility of various organic cations and anions that are hydrogen bond capable and, therefore, have the potential for extended network generation.³

The imidazole molecule displays interesting intrinsic properties. It meets the basic molecular criteria required for non-linear optical materials: a lack of an inversion centre, the presence of a conjugated electron system and the simultaneous existence and interaction of an electron attracting and electron-withdrawing

group. In neutral conditions imidazole can be considered as an acid with a pK_a near 7 which makes it ‘an optimum catalyst and buffer’ in aqueous solution. The single proton donor on N1 is conjugated with the single proton acceptor N3 residing on a neighbouring molecule, so that the donating and accepting abilities of both sites are strongly correlated. This function is well demonstrated in the crystal structure of the unsubstituted imidazole, where glide related molecules, extended *via* N–H···N hydrogen bonds (2.859 Å), form infinite chains oriented along the *c* crystal axis.⁴ Inversion related chains are stacked parallel to the (101) plane with an inter-ring (N1···N1) distance of 3.54 Å. Strong acids usually protonate the imidazole in order to form imidazolium cations, in which the protons on N1 and N3 readily donate hydrogen bonds toward the oxygen sites of the acid anion (Scheme 1).

The imidazolium cation in these systems displays two important features that may be of potential interest for deliberately designed systems. (i) The aromatic character of the ring provides the system with mobile π-electrons; (ii) the internal symmetry relations of the five-membered imidazolium ring requires a twofold rotation axis or a mirror plane through the C2–H2 bond, an important factor for a molecular arrangement without an inversion centre. For example in imidazolium carboxylates the imidazolium ring serves as a linker between the anions in order to extend them into one-dimensional hydrogen-bonded arrays in the case of monoacids or into two-dimensional hydrogen-bonded arrangements in the case of diacids. The chains in the former are always polar, whereas the polarity of the 2D networks in the latter depends upon the chemical nature of the diacid.⁵ On the other hand, the coordination chemistry of phosphonic acids (H₂O₃PR, R = alkyl or aryl group) gains attention mainly for the possibility of designing structures with specific properties. Numerous metal phosphonates of unusual compositional and structural complexity have been synthesized and reported. Their structural



Scheme 1

diversity varies from one-dimensional arrangements⁶ and layered frameworks⁷ to three-dimensional microporous frameworks.⁸ Diphosphonic acids, similar to disulfonic acids⁹ can be used as pillaring agents in the design of pillared three-dimensional structures.¹⁰

Phosphonoacetic acid displays the functions of both carboxylic and phosphonic acids and can be considered as an analogue of malonic acid in which one of the carboxylic groups is replaced with a phosphonic group. Two important consequences issue for the corresponding imidazolium salt. First, the phosphonic group which is more acidic ($pK_a < 2$) than the carboxylic moiety (pK_a of 2.85) protonates the imidazole, and second, the single hydrogen-bond donors and the surplus of hydrogen-bond acceptors on the phosphonic and carboxylic sites permits the design of a two-dimensional hydrogen-bonded network without employing imidazolium linkers. Hereafter we report on the supramolecular architecture of imidazolium phosphonoacetate consisting of a porous anionic framework with cations intercalated in the channels that are created between the anionic moieties.

Experimental

General procedures

The commercially available starting materials were purchased from Aldrich and used without further purification. Spectroscopic grade solvents and deionised water were used for crystallization. The melting points were determined with a Bethius plate and are uncorrected. Powder diffraction measurements were performed on a Philips X'Pert instrument (40 kV, 50 mA, Cu-K α radiation). Solid-state infrared spectra were recorded on a Perkin-Elmer 1600 FTIR spectrometer (4 cm⁻¹ resolution).

Synthesis

The imidazolium phosphonoacetate was synthesized from a reaction mixture of 0.1515 g phosphonoacetic acid dissolved in 15 ml methanol and 0.3 g imidazole dissolved in 15 ml methanol. 5 ml of water was added and the solution was stirred under mild temperature condition for 2 hours and then left in an uncovered beaker to allow crystallization by slow evaporation. Beautiful colourless, prism-like crystals appeared in several days. The product homogeneity was tested by comparing the powder diffraction spectra of the product with those of the starting materials and the melting point measurement (mp 175–177 °C vs. 143–146 °C for the phosphonoacetic acid and 89–91 °C for the imidazole), and characterized by IR spectroscopy (Nujol and fluorolube mulls): ν/cm^{-1} 3177 (sh), 3170, 3140, 3086 2959, 2790, 2987 (sh), 2812, 2762, 2734 (sh), 2650, 2590, 1890, 1694, 1602, 1462, 1377, 1279, 1215, 1187, 1152, 1124, 1103, 1068, 1061, 990, 906, 843, 815, 772, 709, 610. According to expectations, the most prominent IR changes were observed in the regions of the νOH , νNH , $\nu\text{C=O}$ and νPO_3 stretching vibrations, compared with those of the substrates. The shrinking of the νOH mode, the activation of the out-of-plane overtone, the $\nu\text{C=O}$ band narrowing, as well as the significant position shifts and the splitting of the νPO_3 modes correlate well with the modified hydrogen-bonded network of the newly formed solid state pattern.

X-Ray crystallography

The data collections were performed on an Enraf-Nonius CAD-4 diffractometer with graphite-monochromated Mo-K α radiation ($\lambda = 0.71069 \text{ \AA}$) using the ω -scan technique at 297 K. Lattice parameters were obtained from the least squares refinement using the setting angles of 25 carefully centred reflections in the range $26.6 < 2\theta < 55.0^\circ$. The structure was

solved by direct methods with MITHRIL¹¹ and DIRDIF¹² and refined by full-matrix least-squares techniques. The positions of the H atoms attached to the nitrogen and oxygen were located in the difference maps and refined isotropically, whereas the carbon H atoms were included in the structure-factor calculation and placed in idealized positions with assigned isotropic displacement parameters: $B = 1.2B$ of the C atoms to which they are bonded. Lorentz-polarisation and secondary extinction corrections were made. The computer program PLATON¹³ was used to analyse the geometry of the hydrogen-bonding patterns. ORTEP¹⁴ and PLATON were used for the graphical representation of the results.

Crystal data. C₅H₉N₂O₅P, $M = 208.11$, colourless prism (0.60 × 0.50 × 0.50 mm), monoclinic, space group $P2_1/c$, $a = 5.318(1)$, $b = 15.358(2)$, $c = 10.804(2) \text{ \AA}$, $\beta = 95.65(2)^\circ$, $V = 872.2(5) \text{ \AA}^3$, $Z = 4$, $T = 297 \text{ K}$, $D_c = 1.574 \text{ g cm}^{-3}$, $F(000) = 432$, $\mu(\text{Mo-K}\alpha) = 0.297 \text{ mm}^{-1}$; 3525 measured reflections, 2657 unique reflections ($R_{\text{int}} = 0.037$), refinements on F for 2214 observed reflections ($I > 2.00\sigma(I)$) and 135 variable parameters, $R = 0.0500$, $wR = 0.0650$. GOF = 1.88; $\rho_{\text{min/max}} = -0.68, 0.60 \text{ e \AA}^{-3}$.

CCDC reference number 184204.

See <http://www.rsc.org/suppdata/jm/b2/b202064p/> for crystallographic data in CIF or other electronic format.

Results and discussion

Solid-state organization and hydrogen-bonded network

The most important crystallographic data concerning bond distances, angles and intermolecular interrelations are presented in Tables 1 and 2. The chemical structure and the atom numbering of the compound are presented in Fig. 1. Since the main focus of this paper is concentrated on the molecular organization and the anion–cation interplay, molecular structural details of the residues will not be described here, except for some essential modifications in their geometric parameters. Generally the crystal structure of imidazolium phosphonoacetate can be considered as consisting of phosphonoacetate monolayers that are crosslinked by imidazolium moieties. However, the anion–cation organization in the three-dimensional hydrogen-bonded network is quite unique and resembles to some extent the hexagonal structures formed by nitrilotris(methylphosphonates).¹⁶ In fact, the charge redistribution and the consequent ion formation take place in solution. The transfer of the proton from the phosphonic group towards the imidazole entity effects a strong conjugation of its π -electron system with a subsequent contraction of the five-membered aromatic ring. As a result, all ring distances become shorter *versus* those of the neutral imidazole molecule (see Table 1). The correlation of the N–C bond distances (1.321(3) Å for N1–C2 bond and 1.309(3) Å for N3–C2 compared to 1.349 and 1.326 Å, in neutral imidazole) is a manifestation of the similar hydrogen bond donating potential on both nitrogen sites. On the other hand, no essential configurational changes are observed in the acid residue, except for the changes of the torsion angles O1–C6–C7–P and O2–C6–C7–P that are explained by the new directional demands for hydrogen-bond access on the carboxylic site. Generally the P–O and the C–O distances are also changed in order to adapt to the new exclusive phosphonate–phosphonate and carboxylic–phosphonate interactions.

Despite the intricate nature of the crystallization process, it is generally accepted that of primary importance for supramolecular assembly is the hierarchy in hydrogen-bond formation, which is dependent upon the strength of the sites and their stereoelectronic accessibility. So, only two feasible O–H...O interactions are exploited for the arrangement of the anionic residues in order to form the (100) monolayers of a large grid.

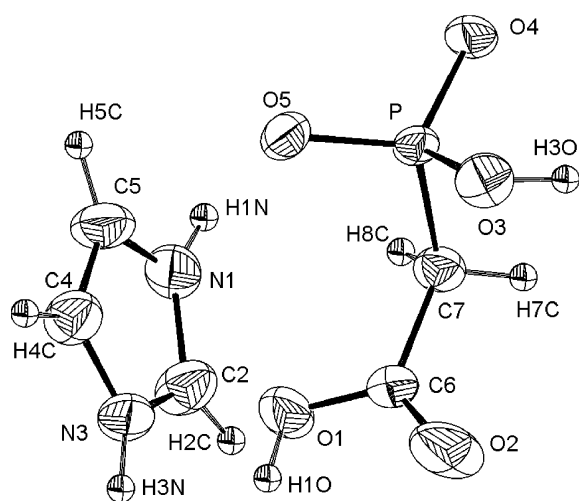
Table 1 Selected intramolecular bond lengths (Å) and angles (°) in the imidazolium phosphonoacetate crystal

	Imidazolium cation	Imidazole molecule ⁴		Imidazolium ion	Imidazole molecule ⁴
N1–C2	1.321(3)	1.349	N1–C2–N3	108.7(2)	111.3
N3–C2	1.309(3)	1.326	C2–N1–C5	108.5(2)	107.2
N1–C5	1.361(3)	1.369	C2–N3–C4	109.1(2)	105.4
N3–C4	1.359(3)	1.378	N1–C5–C4	106.95(19)	106.3
C4–C5	1.347(3)	1.358	N3–C4–C5	107.0(2)	109.8
N1–H1N	0.93(4)	1.048	C2–N1–H1N	134(2)	129.1
N3–H3N	0.86(3)		C5–N1–H1N	117(2)	122.9
	Phosphonoacetate anion	Phosphonoacetic acid ¹⁵		Phosphonoacetate anion	Phosphonoacetic acid ¹⁵
P–O3	1.570(1)	1.544(2)	O3–P–O4	110.78(8)	118.8(1)
P–O4	1.504(1)	1.544(2)	O3–P–O5	106.90(8)	109.3(1)
P–O5	1.503(1)	1.494(2)	O4–P–O5	116.06(7)	107.7(1)
P–C7	1.802(2)	1.799(2)	O1–C6–O2	122.6(2)	122.3(1)
C6–O1	1.297(2)	1.305(2)	P–C7–C6	113.6(1)	114.2(1)
C6–O2	1.194(2)	1.216(2)	O5–P–C7–C6	–54.8(2)	64.5(2)
C6–C7	1.507(2)	1.503(2)	O1–C6–C7–P	96.0(2)	52.0(2)
			O2–C6–C7–P	–83.4(3)	–128.0(2)

Table 2 Hydrogen bond geometry in imidazolium phosphonoacetate

Hydrogen bond interaction	$R(\text{H}\cdots\text{B})/\text{Å}$	$R(\text{A}\cdots\text{B})/\text{Å}$	$\theta(\text{A}-\text{H}\cdots\text{B})^\circ$	Symmetry code	H.B. motif
Anion 2D porous framework – phosphonoacetate hexameric structural module					
(1) O1–H1O \cdots O5	1.76(3)	2.593(2)	165(3)	$x, \frac{1}{2} - y, -\frac{1}{2} + z$	R6,6(32)
(2) O3–H3O \cdots O4	1.73(3)	2.643(2)	171(3)	$-1 - x, 1 - y, 1 - z$	C(6) R2,2(8)
Anion–cation 3D interplay					
(3) N1–H1N \cdots O5	1.79(4)	2.717(2)	168(3)	x, y, z	D
(4) N3–H3N \cdots O4	1.84(3)	2.684(2)	167(3)	$1 + x, \frac{1}{2} - y, -\frac{1}{2} + z$	D
Stabilizing interactions					
(5) C5–H5C \cdots O2	2.472	3.216(3)	135.17	$x, \frac{1}{2} - y, \frac{1}{2} + z$	D
(6) C4–H4C \cdots O2	2.445	3.356(3)	160.14	$-x, -\frac{1}{2} + y, \frac{1}{2} - z$	D
(7) C7–H7C $\cdots\pi$	2.857	3.857	147.36	$-1 - x, \frac{1}{2} + y, \frac{1}{2} - z$	D

Glide-related acid residues are conjoined *via* the strongest carboxylic–phosphonate hydrogen bond O1–H1O \cdots O5 (assigned as 1 in Table 2) and extended into zigzag polar chains along the *c* crystal axis. On the other hand, phosphonate–phosphonate interactions O3–H3O \cdots O4 (assigned as 2) of comparable force are used to traverse the chains running in the opposite direction in the *b* direction (*via* R2,2(8) hydrogen-bonded motif), thus completing the two-dimensional anionic network. Closer insight makes clear that six phosphonoacetate residues belonging to

**Fig. 1** The chemical structure and the numbering scheme of imidazolium phosphonoacetate. Displacement ellipsoids are shown at the 50% probability level (ORTEP3¹⁴).

two neighbouring chains surround the large holes created between the chains. The sizes of the cavities, measured as the interchain O1 \cdots O1 and O3 \cdots O3 distances are 17.6161×10.3446 Å. Therefore, the two-dimensional hydrogen-bonded network can be delineated by the giant R6,6(32) rings (see Fig. 2) that take advantage of six hydrogen bonds: two pairs of parallel carboxylic–phosphonate and two parallel pairs of phosphonate–phosphonate interactions. The phosphonoacetate monolayers are stacked at a unit cell distance of 5.318 Å along the *a* direction in order to form channels (Fig. 3). The imidazolium cations are alternatively arrayed from both sides of the chains *via* N1–H1N \cdots O5 hydrogen bonds (assigned as 3) and fit in the cavities (Fig. 4a). Each two imidazolium residues locked in the cavity protrude up and down from the monolayer and connect to the next monolayer *via* N3–H3N \cdots O4 (assigned as 4). Finally, two weak C–H \cdots O hydrogen bonds (assigned as 5 and 6) and a C–H $\cdots\pi$ interaction (assigned as 7) stabilise the crystal structure fixing the positions of the rings as channel walls. Interestingly enough, there are no stacking or any other aromatic interactions between the imidazolium rings that are intercalated along the *a* axis at a crystal unit cell distance of 5.318 Å (Fig. 4b).

Conclusions

We deliberately synthesized imidazolium phosphonoacetate in an attempt to design an anionic framework with nano-size cavities where cations reside. The analysis of the stereoelectronic and topological predispositions of the sites, as well as the hydrogen bond priorities allowed us to surmise that only two O–H \cdots O hydrogen bonds are adequate for generating this network. We judged the carboxylic hydrogen atom as a

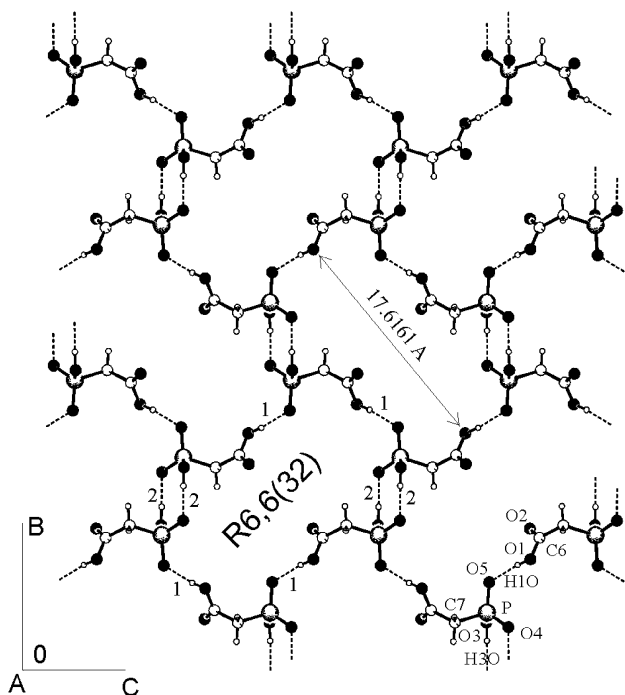


Fig. 2 A view of the 2D hydrogen-bonded anionic network generated *via* hydrogen bonds 1 and 2. The numbering of the hydrogen bonds is consistent with that in Table 2.

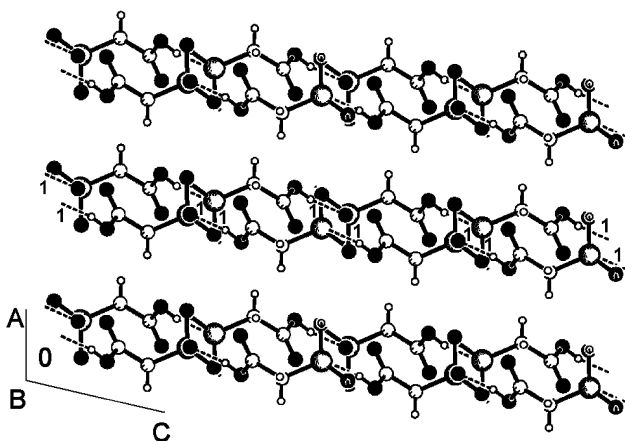


Fig. 3 A side view of the phosphonoacetate monolayers stacked at a unit cell distance along the *a* crystallographic axis. The imidazolium rings are omitted for clarity.

stronger donor than the second hydroxyl hydrogen atom of the phosphonic group (subsequent to the release of the first hydroxyl hydrogen in order to form the imidazolium cation). On the other hand the phosphonate oxygen $O(sp^2)$ was valued as a better acceptor than the carbonyl oxygen of the carboxylic group. In this situation it was not hard to predict that the carboxylic–phosphonate interaction should predominate over the phosphonate–phosphonate and carboxylic–carboxylic interactions. The engagement of the carboxylic hydrogen in the $C-O-H \cdots O=P$ bond should disable any carboxylic–carboxylic connection. No further phosphonate–carboxylic interplay is possible due to topological and steric considerations.

The inclusion of the imidazolium cation in the hollows of the anionic network also was not difficult to imagine taking into consideration the topology of the two proton donors on its nitrogen sites and the possible donating capabilities of the imidazolium carbon sites. Nonetheless, the channel architecture templated by the imidazolium rings was not as obvious at

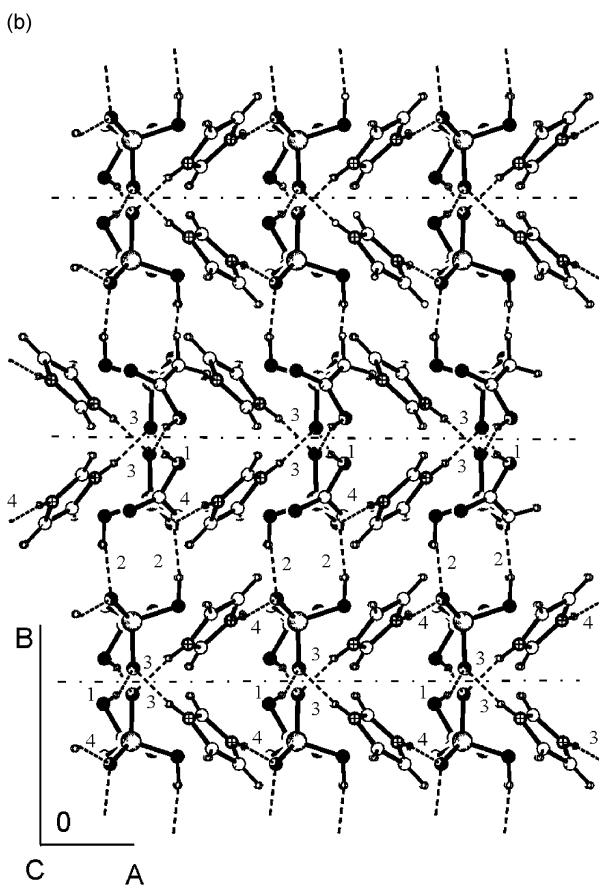
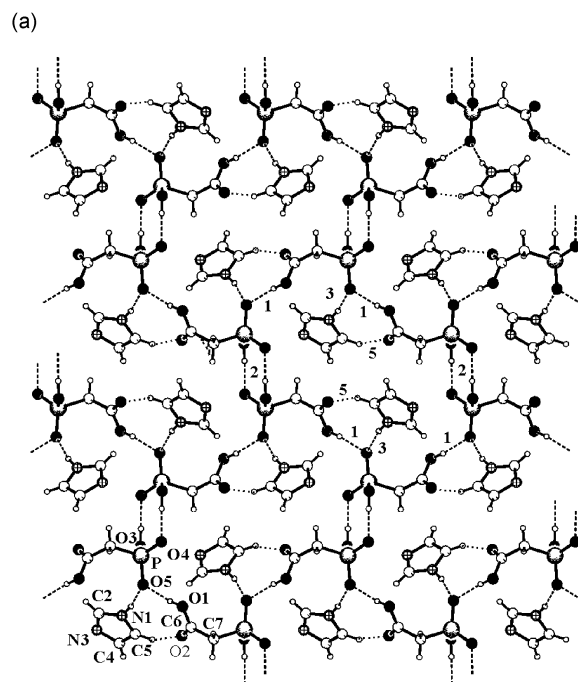


Fig. 4 (a) A presentation of a single (100) monolayer. The imidazolium cations, alternatively arranged *via* the hydrogen-bond numbered as 3 from both sides of the *c* chains, fit in the cavities formed between them. An additional weak hydrogen bond 5 locks the rings inside the hollows encompassed by six anions. (b) A view along the chains demonstrating the organization of the imidazolium rings in the channels: \cdots present the boundaries of the channels.

the starting point of this project, mostly due to the abundance of oxygen sites on the anions. We rather expected the $H3N$ to approach the carbonyl oxygen $O(sp^2)$, which although being the second strongest acceptor cannot participate in the primary

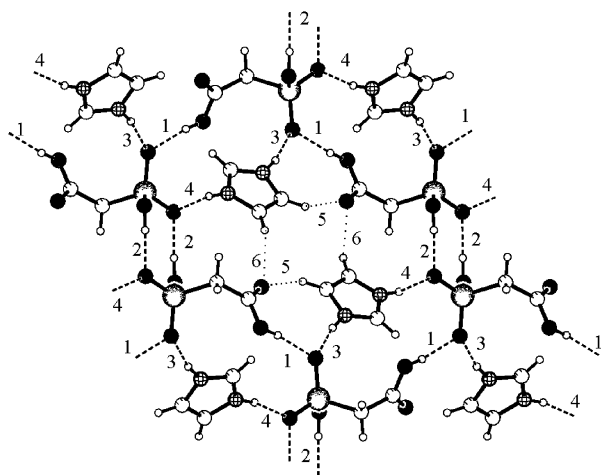


Fig. 5 A view along a single channel. Two pairs of parallel hydrogen bonds 1 and two parallel pairs of hydrogen bonds 2 encircle the cavity. Two imidazolium rings are trapped inside the cavity *via* hydrogen bonds 3 and 5. Two more hydrogen bonds 4 and 6 traverse up or down the cavity to approach the upper and lower hexamers, stabilizing the channel. This module, consisting of three stacked hexamers, bears the complete geometrical, topological and directional information for selective organization and structural recognition.

network for the reasons explained above. However, only after the crystal structure was resolved, it became clear that, due to the rigid configuration of the primary anionic network, the O2 atom is inaccessible for H3N. The decisive role for such and not another type of organization seemed to be played by the weak C–H···O and C–H··· π interactions, that customarily accommodate the directional demands of the network and relax the tension in it. It is worthy to note that the imidazolium H2C atom, which otherwise readily donates hydrogen bonds, is not exploited here since the single lone pairs on both the phosphonate and the carboxylic hydroxyl oxygens are not accessible for it.

Finally, we want to postulate some theories based on our chemical intuition concerning the crystal nucleation process in this crystal. A supramolecular structural module consisting of three stacked hexameric units with 72 hydrogen bonds is presented in Fig. 5. This ‘*mature assembly*’ bears the complete geometrical, topological and directional information for uniform structural recognition in three dimensions. Once formed in solution, it carries the potential to organize the surrounding space *via* selective recognition of only similar assemblies or smaller subunits. The hydrogen-bonding sites on its outer surface are able to bind only those units that approach with an orientation proper to match them and thus to continue to build the ‘*genuine*’ crystal network. Any other subunits and earlier aggregation forms, allowing for multiple recognition and/or structural mistakes are disregarded and progressively eliminated from its close vicinity. In effect, they become less abundant in the solution and therefore, statistically less favoured making the ‘*mature assembly*’ the only preferred form for long-range arrangement. So, this structural unit consisting of eighteen phosphonoacetate and eighteen imidazolium residues seems to be the smallest formation able to direct the crystallization process in solution and can be considered as a *prenuclear phase*, that initiates crystal nucleation.

Acknowledgement

Financial support by the Centre of Nanotechnology and Advanced Materials is gratefully acknowledged.

References

- 1 G. R. Desiraju, *J. Chem. Soc., Dalton Trans.*, 2000, 3745; D. Braga, *J. Chem. Soc., Dalton Trans.*, 2000, 3745; M. J. Zaworotko, *Chem. Commun.*, 2001, 1; K. Biradha, D. Dennis, V. A. MacKinnon, C. V. K. Sharma and M. J. Zaworotko, *J. Am. Chem. Soc.*, 1998, **120**, 11894.
- 2 G. R. Desiraju, *Angew. Chem., Int. Ed. Engl.*, 1995, **43**, 2311; G. R. Desiraju, *Chem. Commun.*, 1997, 1475.
- 3 V. Videnova-Adrabińska, I. Turowska-Tyrk, T. Borowiak and G. Dutkiewicz, *New J. Chem.*, 2001, **25**, 1403; V. Videnova-Adrabińska and E. Janeczko, *J. Mater. Chem.*, 2000, **10**, 555.
- 4 S. Martinez-Carrera, *Acta Crystallogr.*, 1966, **20**, 783; B. M. Graven, R. K. McMullan, J. D. Bell and H. C. Freeman, *Acta Crystallogr., Sect. B*, 1977, **33**, 2585.
- 5 J. C. MacDonald, *PhD Thesis*, University of Minnesota, 1993; I. Karle, D. Ranganathan and V. Haridas, *J. Am. Chem. Soc.*, 1996, **118**, 7128.
- 6 D. Grohol, M. A. Subramanian, D. Poojary and A. Clearfield, *Inorg. Chem.*, 1996, **35**, 5264; D. Grohol and A. Clearfield, *J. Am. Chem. Soc.*, 1997, **119**, 4462; B. L. Bujoli, P. Palvadeau and J. Rouxel, *Chem. Mater.*, 1990, **2**, 582.
- 7 M. D. Poojary, H. L. Hu, F. L. Campbell III and A. Clearfield, *Acta Crystallogr., Sect. B*, 1993, **49**, 996; G. Cao, H. Lee, V. M. Lynch, J. S. Swinnea and T. E. Mallouk, *Inorg. Chem.*, 1990, **29**, 2112; A. Cabeza, M. A. G. Aranda, M. Martinez-Lara, S. Bruque and J. Sanz, *Acta Crystallogr., Sect. B*, 1996, **52**, 982; D. M. Poojary, B. Zhang, P. Bellinghausen and A. Clearfield, *Inorg. Chem.*, 1996, **35**, 4942; A. Cabeza, M. A. G. Aranda, S. Bruque, M. D. Poojary, A. Clearfield and J. Sanz, *Inorg. Chem.*, 1998, **37**, 4168.
- 8 L. J. Bideau, C. Payen, P. Palvadeau and B. Bujoli, *Inorg. Chem.*, 1994, **33**, 4885; S. Drummel, P. Janvier, D. Deniaud and B. Bujoli, *J. Chem. Soc., Chem. Commun.*, 1995, 1051; M. D. Poojary, A. Cabeza, M. A. G. Aranda, S. Bruque and A. Clearfield, *Inorg. Chem.*, 1996, **35**, 1468; M. D. Poojary, D. Grohol and A. Clearfield, *Angew. Chem., Int. Ed. Engl.*, 1995, **34**, 1508; K. Maeda, J. Akimoto, Y. Kiyozumi and F. Mizukami, *Angew. Chem., Int. Ed. Engl.*, 1995, **34**, 1199; K. Maeda, J. Akimoto, Y. Kiyozumi and F. Mizukami, *J. Chem. Soc., Chem. Commun.*, 1995, 1033.
- 9 V. A. Russell, C. C. Evans, W. Li and M. D. Ward, *Science*, 1997, **276**, 575; C. C. Evans, L. Sukarto and M. D. Ward, *J. Am. Chem. Soc.*, 1999, **121**, 320.
- 10 G. Alberti, R. Constantino, F. Marmottini and Z. P. Vivani, *Angew. Chem., Int. Ed. Engl.*, 1993, **32**, 1357; G. Alberti, F. Marmottini, S. Murcia-Mascaros and R. Vivani, *Angew. Chem., Int. Ed. Engl.*, 1994, **33**, 1594; M. E. Thompson, *Chem. Mater.*, 1994, **6**, 1168; D. M. Poojary, B. Zhang, P. Bellinghausen and A. Clearfield, *Inorg. Chem.*, 1996, **35**, 5254; A. H. Mahmoudkhani and V. Langer, *Cryst. Growth Des.*, 2002, **2**, 21.
- 11 C. J. Gilmore, *Appl. Crystallogr.*, 1984, **17**, 42.
- 12 P. T. Buerskens, W. P. Bosman, H. M. Doesburg, R. O. Gold, Th. E. M. Van den Hark, P. A. J. Prick, J. H. Noordick, G. Buerskens, V. Parthasarathi, H. J. Bruins Slot and R. C. Haltiwanger, *DIRDIF: Direct Methods for Difference Structures*, Technical Report 1984/1, Crystallography Laboratory, Toernooiveld, 6525 Ed Nijmegen, The Netherlands, 1984.
- 13 A. L. Speck, PLATON, A Multipurpose Crystallographic Tool, Utrecht University, The Netherlands, 1999.
- 14 L. J. Farrugia, *J. Appl. Crystallogr.*, 1997, **30**, 565.
- 15 T. Lis, *Acta Crystallogr., Sect. C*, 1997, **53**, 28.
- 16 C. V. K. Sharma, A. J. Hessheimer and A. Clearfield, *Polyhedron*, 2001, **20**, 2095.